Separation Science and Technology

ISSN: 0149-6395 (Print) 1520-5754 (Online) Journal homepage: https://www.tandfonline.com/loi/lsst20

Uptake of Fluoride by Al^{3+} Pretreated Low-Silica Synthetic Zeolites: Adsorption Equilibrium and Rate Studies

Maurice S. Onyango , Yoshiro Kojima , Anil Kumar , Dalibor Kuchar , Mitsuhiro Kubota & Hitoki Matsuda

To cite this article: Maurice S. Onyango , Yoshiro Kojima , Anil Kumar , Dalibor Kuchar , Mitsuhiro Kubota & Hitoki Matsuda (2006) Uptake of Fluoride by Al^{3+} Pretreated Low-Silica Synthetic Zeolites: Adsorption Equilibrium and Rate Studies, Separation Science and Technology, 41:4, 683-704, DOI: 10.1080/01496390500527019

To link to this article: https://doi.org/10.1080/01496390500527019

Published online: 15 Feb 2007.

Separation Science and Technology, 41: 683–704, 2006

ISSN 0149-6395 print/1520-5754 online
DOI: 10.1080/01496390500527019

Taylor & Francis
Taylor & Francis Group

Uptake of Fluoride by Al^{3+} Pretreated Low-Silica Synthetic Zeolites: Adsorption Equilibrium and Rate Studies

Maurice S. Onyango
Department of Chemical Engineering, Nagoya University, Furo-cho, Chikusa-ku, Nagoya, Japan

Yoshiro Kojima
Ecotopia Science Institute, Nagoya University, Furo-cho, Chikusa-ku, Nagoya, Japan

Anil Kumar
Department of Chemical and Process Engineering, Moi University, Eldoret, Kenya

Dalibor Kuchar
Department of Chemical Engineering, Nagoya University, Furo-cho, Chikusa-ku, Nagoya, Japan

Mitsuhiro Kubota and Hitoki Matsuda
Department of Energy Engineering and Science, Nagoya University, Furo-cho, Chikusa-ku, Nagoya, Japan

Abstract: The removal of fluoride from single component aqueous solution using Al^{3+}- pretreated low-silica synthetic zeolites (Al-Na-HUD, Al-HUD, Al-F9, and Al-A4) was studied. The effects of adsorbent mass, initial solution pH, and initial concentration on fluoride removal in a batch system were evaluated. Equilibrium data were simulated using simple isotherms such as the Freundlich (F), Langmuir-Freundlich (LF), Redlich-Peterson (RP) and Dubinin-Radushkevitch (DR) isotherms. From the

Received 5 May 2005, Accepted 7 December 2005
Address correspondence to Hitoki Matsuda, Department of Energy Engineering and Science, Nagoya University, Furo-cho, Chikusa-ku, Nagoya 464-8603, Japan. E-mail: matsuda@nuce.nagoya-u.ac.jp

DR model, initial pH effects and desorption studies, it was considered that the fluoride adsorption onto the zeolites proceeded by ion-exchange or chemisorption mechanism. In interpreting the kinetic results, reaction kinetics (using Elovich equation) and mass transfer processes (both external mass transfer and intraparticle diffusion) were considered. Equilibrium and kinetic results of fluoride adsorption onto the adsorbents demonstrated the following order of performance: Al-Na-HUD > Al-F9> Al-HUD > Al-A4.

Keywords: Fluoride, low-silica zeolites, adsorption, equilibrium, kinetics

INTRODUCTION

In recent years, zeolites have gained popularity in liquid-phase adsorption processes. The motivating factors have been among others, their ability to exchange their weakly bound cations with those in solution, their availability in abundance both in natural and synthetic forms and their large internal surface areas. Because zeolites exchange cations easily, a lot of research has mainly focused on their use in removal of heavy metals from contaminated water sources (1–5). Some research however has shown that zeolites can be used in removing anions from water (6, 7). One disadvantage of using zeolites in anions adsorption inheres in their negative zeta potential in solution over wider pH range. The preceding factor (negative charge) results in coulombic repulsive forces between the zeolite surfaces and adsorbing anions. Thus, to effectively use zeolites in anions adsorption, their surfaces need to be tailored in such a manner as to create surface active sites that are efficient and specific to target anions.

Surface modification of zeolites to create new sorption sites that are efficient and specific to target anions is sparsely reported in literature (8–11). In these cases, the target anions are those that are found in solution at concentrations that are detrimental to human health. Most notable among these anionic species are fluoride and arsenic (12). Fluoride of geologic and anthropogenic origins in groundwater and water streams are a major issue in certain parts of the world. When such water is ingested for a period of time, teeth mottling and the less common bone fluorosis may result. At the moment, the World Health Organization (WHO) recommends a maximum allowable concentration of 1.5 mgF/L in drinking water. We have shown in our previous work (8) that by wet method, zeolites can be charged-reversed (become positively charged) with aluminium ions. The process involved ion exchange of zeolite bound sodium with aluminium ions from solution. The aluminium ions specifically adsorbed on the zeolite, altering its electrokinetic property. The equilibrium capacity of the prepared zeolite was shown to be 37–40 mgF/g. This value was several times higher than the capacity of aluminas; La(III)-impregnated alumina (6.3 mgF/g), Y(III)-impregnated alumina (6.1 mgF/g) and activated alumina (3.3 mgF/g) (13).

In this study, we utilize the large internal surface area, hydrophilicity and the ion-exchange ability of low-silica synthetic zeolites to create fluoride adsorption sites by pretreating the zeolites with Al^{3+} ions. Consequently, adsorption characteristics of fluoride onto the Al^{3+}-pretreated low-silica zeolites under varying conditions such as adsorbent mass, initial pH and initial concentration are evaluated. Simple equilibrium models such as the Freundlich (F), Langmuir-Freundlich (LF), Redlich-Peterson (RP), and Dubbinin-Radushkevitch (DR) are employed to simulate the equilibrium data. The model parameters are then obtained and discussed. Though several research works have been presented for fluoride adsorption (13–22), only a handful have considered kinetic analysis, especially the mass transfer processes (16, 18–21). We have therefore carried out a kinetic analysis of the fluoride sorption on the zeolites to generate parameters that are important in preliminary design of adsorption units. The Elovich equation and models applicable to mass transfer processes (external mass transfer and intraparticle diffusion) are considered. For intraparticle diffusion kinetics, an analytical solution of the governing intraparticle diffusion equation is used. The analytical solution assumes a linear isotherm for adsorption in a finite bath.

MATERIALS AND METHODS

Adsorbent Preparation and Characterization

Aluminum pretreated zeolites were prepared for batch studies by adding separately 50 g each of synthetic zeolites F-9 (Na^+ form; Si/Al ratio: 1.23; pore size: 9Å), A4 (Na^+ form; Si/Al ratio: 1; pore size: 3.8 Å), Na-enriched HSZ 300HUD and HSZ 300HUD ((H^+ form; Si/Al ratio: 2.75–3.25) to a 1 L of 0.075 M aluminum sulfate solutions. Preliminary studies showed that a concentration of 0.075 M aluminum sulfate was optimum to ensure zeolite stability and to maximize fluoride removal capability of the zeolite. The F-9 and A4 zeolites used in this study (particle size 0.500–1.180 mm) were supplied by Wako Chemicals, Japan, while HSZ 300HUD zeolite was donated by Tosoh Chemicals, Japan. The mixtures were stirred for 2 days and then washed several times using demineralized water to lower the electrical conductivity. Finally, the modified zeolites were air-dried at room temperature for 2 days and to enhance mass transfer, they were milled to 0.150–0.300 mm size fraction prior to use. The zeolites prepared in this manner are hereafter referred to as Al-Na-HUD, Al-F9, Al-HUD and Al-A4 for zeolites HSZ 300HUD (Na-enriched), F9, HSZ 300HUD and A4, respectively. The exchange of sodium (F-9 and A4) from the zeolite structure with aluminum from the aqueous solution was verified using EDXS (JED 2140-JEOL). At the same time, the electrokinetic properties of the aluminum pretreated zeolites were determined at various pH values by measuring the zeta potential of the zeolite samples using an electrophoretic light scattering

spectrophotometer (ELS-7300K, Otsuka Electronics Co., Japan). From the zeta potential measurements, the pH_{pzc} of each zeolite adsorbent was determined. In addition, physical properties such as the BET surface area of the zeolites were further characterized by nitrogen adsorption-desorption.

Fluoride Uptake Experiments

In the first set of experiments, the effect of adsorbent mass on fluoride removal from water was studied by varying the amount of each adsorbent from 0.05 g to 0.20 g without solution pH adjustments. Next, the effect of the initial solution pH on fluoride uptake was studied by varying the pH within the range of 2 to 11 using either 0.1 M NaOH or HCl. For this case, the adsorbent mass was fixed at 0.05 g. To obtain data for the construction of fluoride adsorption isotherms, a fixed amount (0.1 g) of the adsorbents was contacted with fluoride-containing aqueous solution. The initial fluoride content of the aqueous solution was varied from 5 to 80 mg/L. In all of the above cases, 50 mL solutions were pipetted into 100 mL plastic bottles. The bottles were placed in a thermostat shaker containing a 298 K water bath and were shaken at 150 strokes per minute (spm) for 2 days. At the end of the experiment, samples were withdrawn from the test bottles and filtered through a 0.2-μm syringe filter and residual fluoride concentration was measured by a fluoride-ion-selective electrode (Horiba, Japan) according to the Japanese Standard Method (JIS K0102). Accordingly, a calibration curve was initially prepared by recording potential values for a range of known fluoride concentration, mostly 0.1–5.0 mg/L. To ensure that other ions did not interfere with the fluoride measurements, Total Ionic Adjustment Buffer solution (TISAB, pH 5.3) containing 58 g NaCl, 1 g diammonium hydrogen citrate, 50 mL acetic acid and an appropriate amount of 5M NaOH all in a volume of 1 L was prepared and used during fluoride ions concentration measurements. The equilibrium adsorption capacity, q_e, was determined from

$$q_e = \frac{C_o - C_e}{\rho} \tag{1}$$

where C_o and C_e are the initial and equilibrium bulk-phase fluoride concentrations, respectively, and ρ is the ratio of adsorbent mass to adsorbent-free volume.

In the final fluoride uptake experiments, short-term kinetic studies were carried out in a 1 L stirred tank batch adsober operated at about 298 K to analyze the mechanism of reaction and transport in fluoride uptake. The effect of zeolite type (Al-Na-HUD, Al-HUD, Al-F9 and Al-A4) on fluoride adsorption kinetics using uniform grain fraction of 0.150–0.300 mm at initial fluoride concentration of 10 mg/L was studied. The 10 mg/L was chosen to be typical of concentration of fluoride found in natural systems

such as groundwater. At time zero and at selected time intervals thereafter (up to 4 hours), 5 mL samples were taken and filtered through a 0.2 μm cellulose acetate filters. For the purpose of reproducibility of the results, the experiments were done in replicates and the results reported are averages of the experimental data. The average amount of fluoride adsorbed at any time, q_t, was calculated from

$$q_t = \frac{C_o - C_t}{\rho} \tag{2}$$

where C_t is the bulk-phase fluoride concentration.

Desorption Studies

The desorption of fluoride loaded on zeolite particles was done using acetic acid, demineralized water, sodium bicarbonate, and sodium hydroxide as desorbing agents. The fluoride contents of the zeolites were 20.6, 16.8, 19.4 and 11.8 mgF/g for Al-Na-HUD, Al-HUD, Al-F9, and Al-A4 zeolites, respectively. Initially, only fluoride loaded Al-F9 adsorbent was tested in an attempt to choose the best desorbing agent. A fixed amount (0.1 g) of the adsorbent was contacted separately with 50 mL of acetic acid, demineralized water, sodium bicarbonate, and sodium hydroxide solutions contained in 100 mL plastic bottles. The bottles were placed in a thermostatic shaker and shaken for 1 day at 150 spm. Sodium bicarbonate was found to be the most effective desorbing agent. Consequently, the desorption of all other zeolite types loaded with fluoride was done using sodium bicarbonate according to the procedure described above. Up to 4 desorption steps were used.

RESULTS AND DISCUSSION

Adosrbents Physico-Chemical Properties

Low-silica zeolites contain a relatively high number of exchangeable cations (sodium or hydrogen in this study), because of which, the surface charge properties of these zeolites can easily be altered and the zeolites can then be used in anions adsorption. This was achieved by exchanging the loosely bound cations with Al^{3+} ions. The alteration in surface charge properties is also a result of specific adsorption of Al^{3+} on the O-plane in the stern layer and the creation of defects in zeolite by the activating solution. From electrokinetic studies (Table 1), the pH_{pzc} values of the Al^{3+}-pretreated zeolites were 6, 6.5, 7.5, and 8.2 for zeolite Al-A4, Al-HUD, Al-Na-HUD, and Al-F9, respectively, giving an indication that the zeolites were positively charged at acidic and near neutral pH range. The exchange of Na-bound zeolite with Al^{3+} ions was verified using EDXS. Several EDXS spectra were taken but only

Table 1. Selected zeolite adsorbent characteristics

Adsorbents	Al-Na-HUD	Al-HUD	Al-F9	Al-A4
Form (before treatment)	H^+	H^+	Na^+	Na^+
Silica/Alumina ratio[a]	2.75–3.25	2.75–3.25	1.23	1
BET surface area (m^2/g)	642.2	1054	231.7	20.7
pH in water	4.3	4.5	5.3	5.8
pH_{pzc}	7.5	6.5	8.2	6.0
Effective amount of aluminum exchanged (mg/g-adsorbent)[c]	negligible	negligible	46.2	8.2
Composition of major elements mol %[b]				
oxygen	63.05 (63.88)	63.16 (63.88)	56.83 (57.06)	55.83 (58.98)
sodium	0 (0.21)	0 (0.21)	3.45 (10.58)	4.22 (11.95)
aluminum	15.29 (16.19)	16.18 (16.19)	19.42 (14.14)	20.0 (16.45)
silicon	21.66 (19.76)	20.51 (19.76)	20.30 (18.22)	19.95 (17.62)

[a]values from the manufacturer (before Al^{3+} pretreatment).

[b]The values in parenthesis for elemental composition denote 'before treatment'.

[c]Effective amount of aluminum exchanged is based on the final concentration of aluminum in solution after pretreatment.

representative spectra for A4 and Al-A4 zeolites are shown in Fig. 1a and 1b. The spatial distributions in regions of micron dimensions of major elements (oxygen, sodium, aluminum and silicon) are also shown. The elements were identified according to the kiloelectron voltage (keV) at which their peaks appeared. For oxygen, the peak appeared at 0.52 keV, while for sodium, aluminium and silicon, the peaks appeared at 1.04, 1.49 and 1.74 keV, respectively. It is observed that the sodium content of zeolite was significantly altered when the zeolite particles were contacted with Al^{3+} ions. Similar results were also found when F9 zeolites was pretreated with Al^{3+}. In the case of HSZ 300HUD, the sodium content was quite low since it was in the H^+ form. The elemental composition and other physical properties of the zeolites are summarized in Table 1. Allowing for experimental error, the elemental composition of Al-HUD and Al-Na-HUD seems to be the same. Moreover, the effective exchange of Al^{3+} (exchange of aluminum with the cations bound on zeolite minus the aluminum leached from the zeolite structure) was negligible.

Effect of Adsorbent Mass

Four different Al^{3+}- pretreated low silica zeolites (Al-Na-HUD, Al-HUD, Al-F9, and Al-A4) have been selected for the purification of fluoride containing

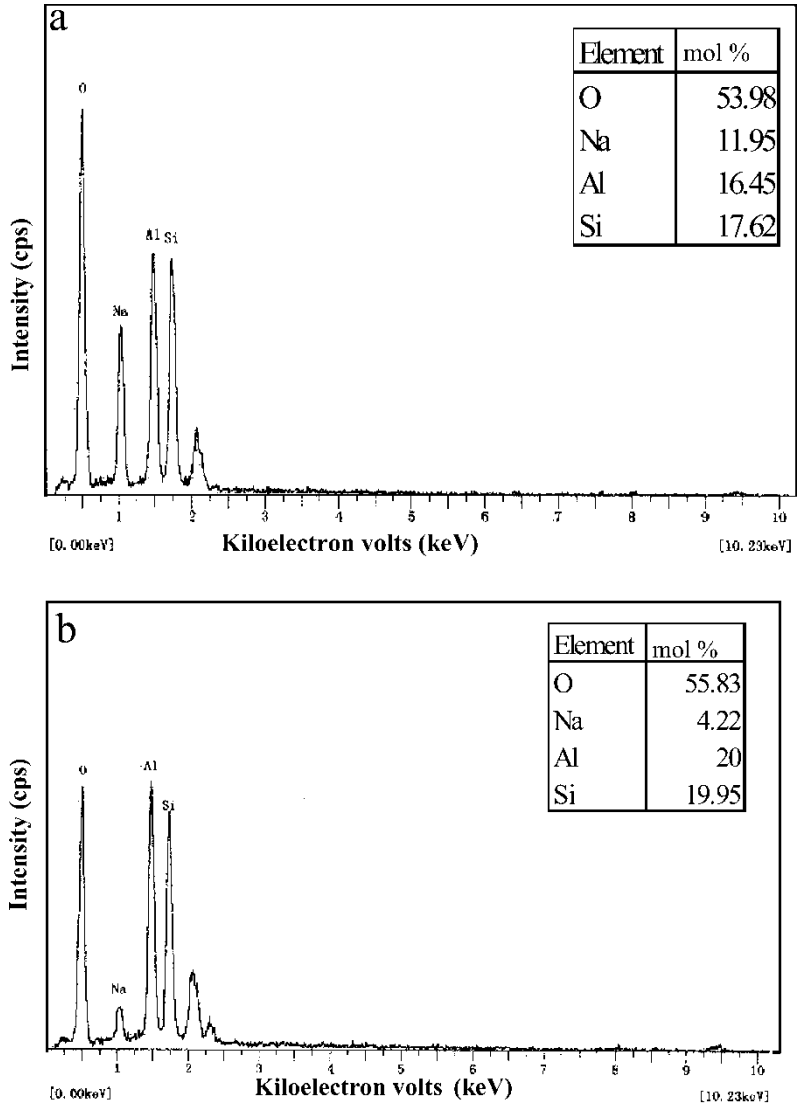

Figure 1. Energy dispersive X-ray spectrometry (EDXS) spectra of (a) A4 zeolite; (b) Al^{3+}-pretreated A4 zeolite (Al-A4).

water. The results of the residual fluoride concentration against amounts of different zeolites are shown in Fig. 2. The residual fluoride concentration decreased with an increase in amount of adsorbent due to increase in ligand exchange sites. From an initial concentration of 10 mg/L, the zeolites were able to remove fluoride to concentrations below 1.5 mg/L, which is the current maximum allowable concentration (MAC) of fluoride in drinking

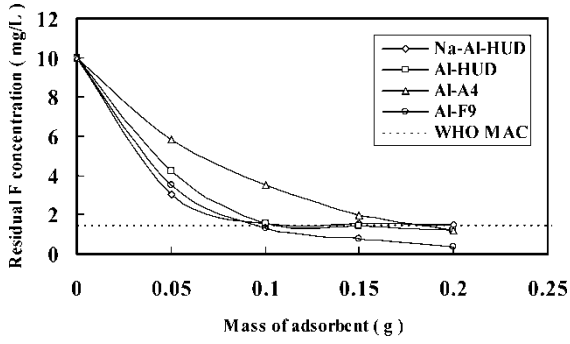

Figure 2. Effect of adsorbent mass on fluoride uptake.

water. The fluoride removal capacity of the zeolites did not follow the trend in their Si/Al ratio, which determines to some extent the number of terminal Al-OH sites. Consequently, the structure and electrokinetic properties of the zeolites could have been the driving force behind their different capacities for fluoride. Meanwhile, the high efficiencies achieved in this work may be due to a higher concentration of terminal Al−OH sites in low Si/Al ratio zeolites, which leads to a greater capacity for a ligand exchange reaction (6).

Effect of pH

One of the factors from solution chemistry that influences the adsorption process is the solution pH. In natural systems such as groundwater, pH value of water varies from point to point. A study was therefore undertaken to ascertain to what extent the initial solution pH affected the adsorption of fluoride onto the low-silica zeolites. Figure 3 shows the effects of initial solution pH on the uptake of fluoride. The uptake of fluoride for each zeolite is relatively constant between pH 4 and pH 8. The magnitude of

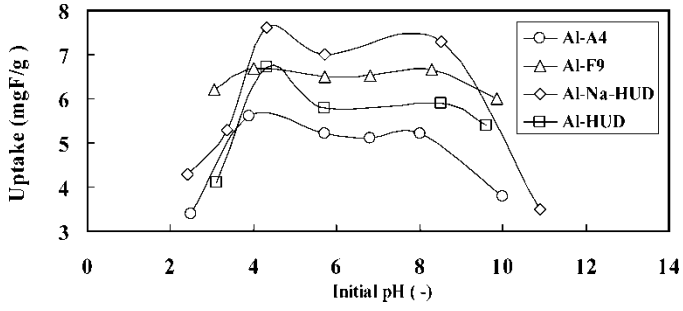

Figure 3. Effect of initial solution pH on fluoride uptake. Initial fluoride concentration = 10 mg/L,adsorbent dose = 1 g/L.

uptake in this pH range follows the order Al-Na-HUD > Al-F9> Al-HUD> Al-A4. Zeolites have been recognized to buffer solution pH (6, 8, 10). When the initial solution pH was fixed in the pH range of 4–8 in this study, the system (solution–adsorbent) pH at equilibrium was buffered in the pH range 6.0–6.8. The buffering effect was responsible for the constant uptake of fluoride by each adsorbent in the pH range of 4–8. Moreover, the buffered pH range lies within the region where fluoride adsorption to aluminol surface sites is reported to be optimum (20).

To further understand the fluoride adsorption behavior under different pH values, the following reactions are considered

$$HF \Longleftrightarrow H^+ + F^- \tag{3}$$

$$Zeo - AlOH + H^+ \Longleftrightarrow Zeo - AlOH_2^+ \tag{4}$$

$$Zeo - AlOH + OH^- \Longleftrightarrow Zeo - AlO^- + H_2O \tag{5}$$

$$Zeo - AlOH_2^+ + F^- \Longleftrightarrow Zeo - AlF + H_2O \tag{6}$$

$$Zeo - AlOH + F^- \Longleftrightarrow Zeo - AlF + OH^- \tag{7}$$

where Zeo-AlOH, Zeo-$AlOH_2^+$, Zeo-AlO^-, and Zeo-AlF are the neutral, protonated and deprotonated aluminol sites and aluminol site-fluoride complex, respectively. Equation (3) expresses the ionization of HF in solution at low pH. Because HF is weakly ionized in solution at low pH values, the corresponding uptake of fluoride is reduced as shown in Fig. 3. When the adsorption system (fluoride solution/zeolite) is operated in the near neutral pH range, reactions expressed in Eqs. (4), (6), and (7) are favored leading to a higher uptake of fluoride. At the same time, the complex interplay between these reactions and the zeolites properties such as their pH in water determines the equilibrium pH (buffered pH value). At high pH values, the aluminol sites are deprotonated according to Eq. (5) leading to a reduction in fluoride adsorption due to increased repulsive forces between the negatively charged fluoride ions and the deprotonated sites. The trends observed in this study where fluoride is removed from solution even at pH above pH_{pzc} of the adsorbents suggest a chemisorption mechanism.

Adsorption Isotherms

Experimental data of fluoride adsorption onto Al^{3+}-pretreated low-silica synthetic zeolites at 298 K are shown in Fig. 4. The data were fitted to the Freundlich (F), Langmuir- Freundlich (LF), Redlich-Peterson (RP), and Dubbinin-Radushkevitch (DR) models (8–11) by linear regression technique as shown in Figs. (5–8), respectively, to determine the best fitting isotherm(s) and the corresponding parameters.

We have hypothesized that the fluoride adsorption sites for the zeolites used in this study may have consisted of protonated and neutral aluminol sites. These sites have different affinities for fluoride and thus, the heat of

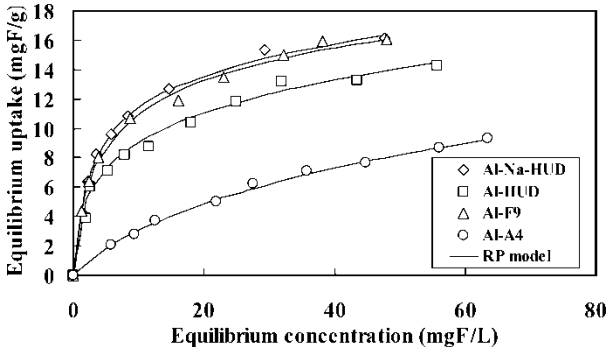

Figure 4. Equilibrium fluoride uptake by zeolite adsorbents at 298 K.

adsorption on these sites varies from site to site. Therefore, experimental data were fitted to Freundlich isotherm model Eq. (8) as shown in Fig. 5. Linear plots were obtained with regression coefficients ranging from 0.97 to 0.99. The Freundlich isotherm parameters are summarized in Table 3. The parameter related to adsorption capacity (K_F) decreased in the order Al-Na-HUD > Al-F9 >Al-HUD >Al-A4 on the one hand while on the other hand the heterogeneity coefficient ($1/n$) decreased in the order Al-A4 > Al-F9 > Al-HUD ≈ Al-Na-HUD. From the $1/n$ values (less than 1), it is inferred that all the adsorbents were, to a certain extent, heterogeneous. In order to improve the fitting of the Langmuir and Freundlich isotherms, three-parameter models, Redlich–Peterson (RP) and Langmuir–Freundlich (LF), are often used. Thus, we tested the LF and RP models in their linearized forms as expressed in Eqs. (9) and (10), respectively, and shown in Figs. 6 and 7. When plotting the three-parameter models, a trial and error method was used to optimize the regression coefficient. The parameters and regression coefficients extracted from these plots are summarized in Table 3. For

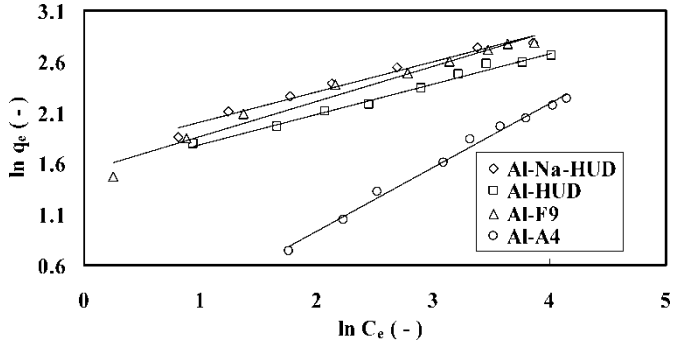

Figure 5. The Freundlich equilibrium isotherm plots for fluoride uptake.

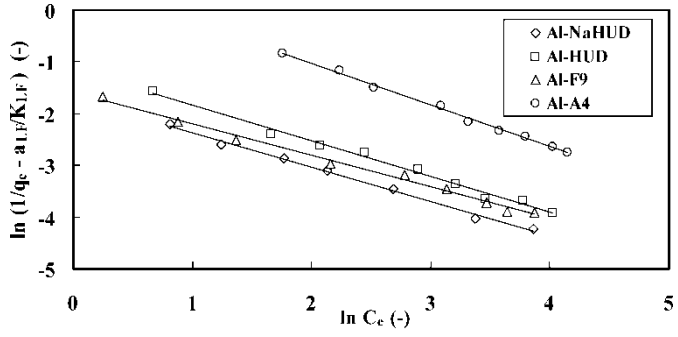

Figure 6. The Langmuir-Freundlich equilibrium isotherm plots for fluoride uptake

example, the LF model parameters K_{LF}, a_{LF} and $1/n$ and regression coefficient R^2 for Na-Al-HUD/fluoride interaction were 5.53, 0.26, and 0.66 and 0.995 while the RP parameters K_{RP}, a_{RP} and β and regression coefficient for the same interaction were 7.66, 0.83, 0.84, and 0.999, respectively. These models also confirm the non-linearity of the zeolite/fluoride interaction since $0 < 1/n < 1$ and $0 < \beta < 1$.

To distinguish the mechanisms involved in fluoride uptake by the four adsorbents, we applied the Dubinin–Radushkevitch (DR) isotherm model, which is based on the Polanyi theory. In its widely used form, it relates the fractional coverage to the Polanyi potential (ε) as given in Eq. (11). For liquid-phase adsorption, $\varepsilon = RT\ln[1 + (1/C_e)]$ where R is the universal gas constant and T the absolute temperature.

Figure 8 shows the plot of ln q_e vs ε^2, from Eq. (11), for the uptake of fluoride by Al^{3+}- pretreated low-silica zeolites at 298 K. Linear curves were obtained whose negative slopes (K) and intercepts ($\ln q_m$) are, respectively, 0.0032, 0.0033, 0.0033, and 0.0074 mol^2/kJ^2 and 3.548, 3.537, 3.340, and 3.722 for Al-Na-HUD, Al-F9, Al-HUD, and Al-A4 zeolites. From the preceding $\ln q_m$ values, the maximum fluoride adsorption capacities, q_m, for

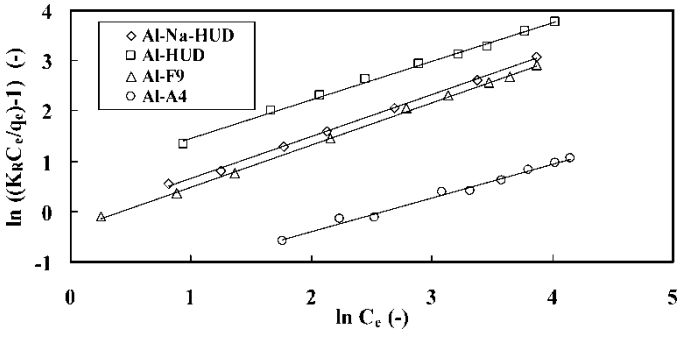

Figure 7. The Redlich-Peterson equilibrium isotherm plots for fluoride uptake.

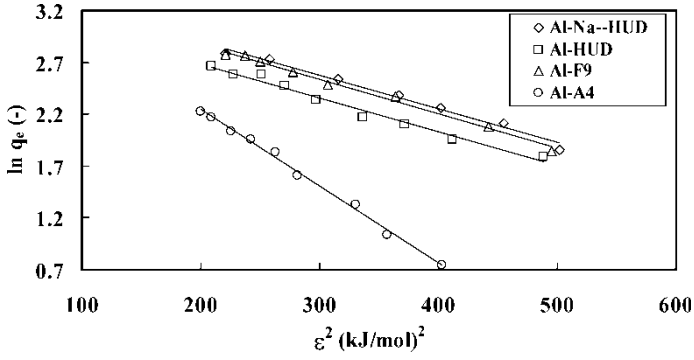

Figure 8. The Dubinin-Radushkevitch equilibrium isotherm plots for fluoride uptake.

Al-Na-HUD, Al-F9, Al-HUD, and Al-A4 zeolites were 34.75, 34.36, 28.21, and 41.35 mg F/g, respectively. The relatively high value predicted for the Al-A4/fluoride adsorption system is due to the shape of the equilibrium curve. To evaluate the nature of interaction between fluoride and the binding sites, mean free energy of adsorption ($E = (2K)^{-0.5}$) per mole of the adsorbate, which is the energy required to transfer one mole of fluoride to the zeolite surface from infinity in solution, was determined. If the magnitude of E is between 8 and 16 kJ/mol, the adsorption process proceeds by ion exchange, while for values of $E < 8$ kJ/mol, the adsorption process is of a physical nature (16). The free energies of adsorption of fluoride onto Al-Na-HUD, Al-F9, Al-HUD and Al-A4 zeolites were 12.5, 12.3, 12.3, and 8.22 kJ/mol, respectively, suggesting that the interaction between fluoride and the zeolites proceeded by ion exchange. Literature also reports that fluoride interaction with aluminol sites involves ligand exchange between fluoride and hydroxyl ions and complexation (23).

Since all the regression coefficients obtained from the F, LF, RP, and DR isotherm models were quite high, normalized standard deviation was used to quantify the noise produced between the experimental and predicted data and to determine the best fitting model(s). The normalized standard deviation (Δq %) is given by

$$\Delta q = 100\sqrt{\frac{\sum((q_{\text{exp}} - q_{cal})/q_{\text{exp}})^2}{N-1}} \tag{12}$$

where q_{exp} is the experimental fluoride uptake, q_{cal} is the calculated amount of fluoride adsorbed and N is the number of data points. The Δq values are summarized in Table 3, from where it can be inferred that the LF and RP isotherm models provide the best correlation between experimental and predicted data.

Table 2. Summary of equilibrium models

Isotherm name	Isotherm model	Linear form	Equation no.
Freundlich (F)	$q_e = k_F C_e^{\frac{1}{n}}$	$\ln q_e = \ln K_F + \frac{1}{n} \ln C_e$	(8)
Langmuir-Freundlich (LF)	$q_e = \frac{K_{LF} C_e^{1/n}}{1 + a_{LF} C_e^{1/n}}$	$\ln\left[\frac{1}{q_e} - \frac{a_{LF}}{K_{LF}}\right] = \ln K_{LF} - \frac{1}{n} \ln C_e$	(9)
Redlich-Peterson (RP)	$q_e = \frac{K_{RP} C_e}{1 + a_{RP} C_e^{\beta}}$	$\ln\left[\frac{K_{RP} C_e}{q_e} - 1\right] = \ln a_{RP} + \beta \ln C_e$	(10)
Dubinin- Radushkevitch (DR)	$\frac{q_e}{q_m} = \exp(-K\varepsilon^2)$	$\ln q_e = \ln q_m - K\varepsilon^2$	(11)

K_F, K_{LF}, K_{RP}: Freundlich, Langmuir–Freundlich, and Redlich–Peterson constants (L/g). a_{LF} a_R: affinity coefficients (L/mg F). $1/n$ or β: heterogeneity coefficient [—]. ε: Polanyi potential (kJ/mol). K: constant (mol^2/kJ^2).

Table 3. Equilibrium modeling parameters for fluoride uptake by zeolite adsorbents

	Parameters				
Zeolite type	$K_{F,LF,RP}$	$1/n$ or β	$a_{L,LF,RP}$	R^2	$\Delta q\%$
Freundlich					
Al-Na-HUD	5.50	0.30	—	0.970	24.6
Al-F9	4.57	0.34	—	0.974	7.5
Al-HUD	4.42	0.30	—	0.988	13.5
Al-A4	0.73	0.62	—	0.992	4.5
Langmuir–Freundlich					
Al-Na-HUD	5.53	0.66	0.26	0.995	2.5
Al-F9	4.93	0.61	0.21	0.993	3.7
Al-HUD	3.19	0.68	0.16	0.990	8.4
Al-A4	0.57	0.80	0.03	0.996	3.2
Redlich–Peterson					
Al-Na-HUD	7.66	0.84	0.83	0.999	2.5
Al-F9	6.47	0.84	0.71	0.999	2.6
Al-HUD	11.30	0.76	2.00	0.997	3.9
Al-A4	0.57	0.67	0.18	0.988	3.3
Dubinin–Radushkevitch					
	q_m	E (kJ/mol)	R^2	Δq %	
Al-Na-HUD	34.75	12.50 (ion exchange)	0.985	23.1	
Al-F9	34.37	12.31 (ion exchange)	0.992	8.2	
Al-HUD	28.12	12.31 (ion exchange)	0.983	11.3	
Al-A4	41.35	8.22 (ion exchange)	0.996	3.3	

Adsorption Rate Studies

The success of an adsorption technology is dictated upon by the availability of a non-toxic and cheap adsorbent of known kinetic parameters and adsorption nature. Moreover, studies on adsorption kinetics in water treatment are important in providing valuable insights into the mechanism of adsorption reaction. In addition, adsorption technology for fluoride removal from water sources is only economical when fluoride exists at low concentrations. Coincidentally, natural systems such as groundwater used as a source of drinking water contains fluoride at low concentrations. Thus, in this kinetic analysis, an initial fluoride concentration of 10 mg/L was taken as a representative value. Experimental kinetic data are shown in Fig. 9 for the adsorption of fluoride ions onto Al-Na-HUD, Al-F9, Al-HUD, and Al-A4 zeolites. It is observed that the uptake depends on the zeolite type and increases with time. There are three main steps in fluoride adsorption onto Al^{3+}-pretreated zeolites. These are diffusion of fluoride ions from bulk liquid-phase to the

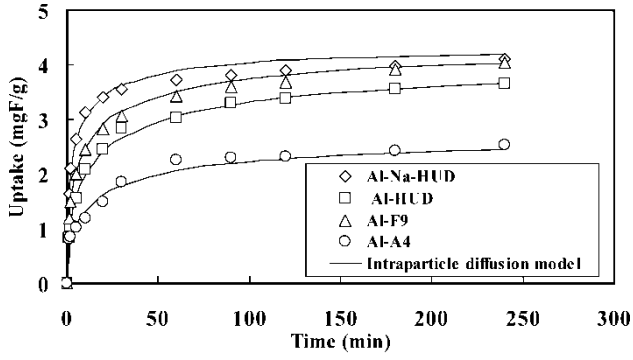

Figure 9. Effect of zeolite type on the uptake of fluoride at various time values (solid lines indicate intraparticle diffusion modeling). Initial fluoride concentration = 10 mg/L, adsorbent dose = 2 g/L, agitation speed 300 rpm.

zeolite surface (film diffusion), internal diffusion in the pores and along the surfaces (intraparticle diffusion), and final adsorption step (chemisorption). These steps form the basis of the succeeding kinetic modeling and analysis.

The Elovich Kinetic Modeling

As already mentioned, both the protonated and neutral aluminol surface sites Eqs. (6) and (7) are the fluoride adsorption sites. Fluoride interaction with these sites involves the formation of strong bonds (chemisorption) but the sites have different affinities for fluoride. In the present adsorption system, the Elovich kinetic model is used to interpret the final adsorption step. The Elovich kinetic model was initially applied to gas-phase adsorption. Recently, it has been successfully used to characterize liquid-phase adsorption kinetics as evident from the works of Cheung et al. (24) House et al. (25), and Lazaridis and Asouhidou, (26), among others. The rate law is based on the premise that chemisorption energies are influenced by adsorbent surface coverage. Alternatively, the active sites are spatially heterogeneous in nature and exhibit different activation energies for chemisorption (27). In the Elovich rate law, the rate of adsorption which is taken as the rate of formation of surface complexes, exponentially decreases with increasing coverage q_t (28):

$$\frac{dq_t}{dt} = a\exp(-bq_t) \tag{13}$$

where a is a parameter defining the rate of chemisorption at zero coverage and b is a parameter related to the extent of surface coverage. Integrating

Eq. (13) subject to the boundary conditions t = 0 to t = t and $q_t = 0$ to $q_t = q_t$ gives an equation in the form

$$q_t = \frac{1}{b}\ln(1 + abt) \tag{14}$$

Introducing a time constant $t_o = 1/ab$, leads to a linearized equation in the form

$$q_t = \frac{1}{b}\ln(ab) + \frac{1}{b}\ln(t + t_o) \tag{15}$$

The fitting validity of the Elovich equation was tested by plotting q_t against $\ln(t + t_o)$. The time constant, t_o, was used as a fitting parameter. Figure 10 shows the Elovich kinetic plots based on Eq. (15). The linear plots are highly significant with regression coefficients above 0.99 except for A1-A4 zeolite. However, Al-Na-HUD/fluoride adsorption system shows dual linearity. The Elovich parameters a and b were obtained from the slope and intercepts of these linear plots and are summarized in Table 4.

When the initial fluoride concentration was fixed at 10 mg/L, the magnitude of the parameter a was in the order Na-Al-HUD > Al-F9 > Al-HUD > Al-A4, indicating that the initial uptake of fluoride ions was fastest in Na-Al-HUD/fluoride adsorption system. Overall, the large values of a obtained in this work are an indication of the rapidity with which fluoride was bound on the zeolites at near time zero. The dependence of initial uptake rate, a, on zeolite type may have been due to differences in the surface chemistry of the zeolites leading to variation in initial attractive force for fluoride ions. Meanwhile, parameter b was relatively constant except for A4. Considering the quantities of fluoride adsorbed after 240 minutes; 3.65, 4.05, and 4.10 mgF/g for Al-HUD, Al-F9, and Na-Al-HUD zeolites, respectively, it is not surprising that b parameter is relatively constant for the three zeolites, since this parameter is related to surface coverage.

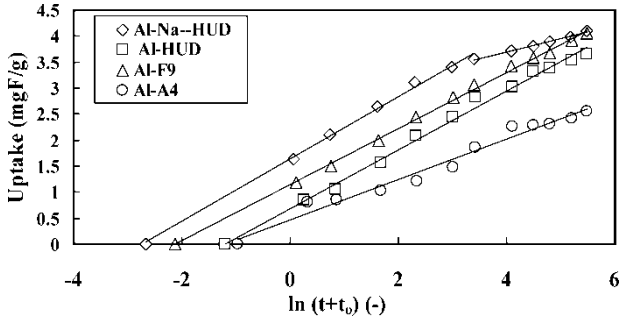

Figure 10. Elovich kinetic plot based on Eq. (15).

Table 4. Summary of reaction kinetic and mass transfer parameters

Adsorbents	Elovich kinetic parameters				
	a (mgF/g min)	b (g/mgF)	t_o (min)	R^2	Δq%
Al-Na-HUD[a]	8.83	1.63	0.07	0.997	1.6
Al-F9	4.35	1.84	0.12	0.998	2.1
Al-HUD	1.97	1.78	0.28	0.994	4.8
Al-A4	1.27	2.58	0.30	0.976	11.2
	Mass transfer parameters				
	K_f (cm/s)	D_e (cm^2/s)	N_{Bi} (−)	Δq%	
Al-Na-HUD	3.75×10^{-2}	1.12×10^{-9}	3.79×10^{5}	3.0	
Al-F9	1.85×10^{-2}	5.27×10^{-10}	3.97×10^{5}	1.5	
Al-HUD	8.38×10^{-3}	6.14×10^{-10}	1.54×10^{5}	3.3	
Al-A4	5.41×10^{-3}	6.15×10^{-10}	9.95×10^{4}	6.9	

[a]Only parameters for the first linear step are provided.

Mass Transfer Processes

Though the Elovich kinetic model fits the kinetic data extremely well, it is argued that mass transfer processes are in most cases the limiting steps in adsorption process. Thus, an analysis of mass transfer processes was carried out. The evaluation of external resistance to mass transfer was done by first determining the film diffusion coefficients according to a simple method proposed by Mckay (29). The method involves the calculation of the initial slope of the concentration against time curve and substituting the obtained value into Eq. (16)

$$\left.\frac{d(C_t/C_o)}{dt}\right|_{t=0} = -k_f S_A \tag{16}$$

where k_f is the film diffusion coefficient (cm/s) and S_A is the specific surface area of the zeolites (cm^{-1}). The specific surface area is expressed as

$$S_A = \frac{6m_s}{\rho_p d(1-\varepsilon_p)} \tag{17}$$

where m_s is the zeolite mass per unit volume (g/cm^3), ρ_p is the density of zeolite (g/cm^3), d is the average zeolite size and ε_p is the porosity.

The film diffusion coefficients determined according to Eq.(16) are summarized in Table 4. The k_f values follow the trend Na-Al-HUD > Al-F9 > Al-HUD > Al-A4 and the magnitude is in the range 10^{-2}–10^{-3} cm/s. This range of k_f values is high implying less external resistance to mass transfer. Moreover, they are comparable to those reported by Mahramanlioglu et al. (16) and Ghorai and Pant (18) for fluoride adsorption on spent bleaching

earth and activated alumina, respectively, and indicates the rapidity with which fluoride ions were transported to the external surface of the zeolites.

In general, as an adsorbate is transported in the internal matrix of an adsorbent, there is a tendency of adsorbate-adsorbate interaction in the pores and hopping, from site to site, of adsorbed species along the wall of the adsorbent. These phenomena give rise to pore and surface diffusion resistances to intraparticle mass transfer. Thus, a parallel pore-surface diffusion model for a differential radial shell of zeolite adsorbent is given by

$$\varepsilon_p \frac{\partial c}{\partial t} + \rho_p(1-\varepsilon_p)\frac{\partial q}{\partial t} = D_p\varepsilon_p \frac{1}{r^2}\frac{\partial\left(r^2\dfrac{\partial c}{\partial r}\right)}{\partial r} + \rho_p D_s \frac{1}{r^2}\frac{\partial\left(r^2\dfrac{\partial q}{\partial r}\right)}{\partial r} \tag{18}$$

where c and q are pore-phase and adsorbed-phase concentrations, respectively, D_p and D_s are the pore and surface diffusion coefficients, ε_p is the particle porosity, ρ_p is the particle density, r is the radial dimension and t is the time. In this model it is assumed that a local equilibrium exists between the adsorbing fluoride ions and those in pore phase for $0 \le r \le r_o$. This local equilibrium for low concentration is described by linear isotherm

$$q = Kc \quad 0 \le r \le r_o \tag{19}$$

Combining Eq. (18) and Eq. (19) and by making several mathematical manipulations leads to

$$\frac{\partial q}{\partial t} = D_e \frac{1}{r^2}\frac{\partial\left(r^2\dfrac{\partial q}{\partial r}\right)}{\partial r} \tag{20}$$

where D_e is the effective diffusion coefficient and

$$\left(\frac{\varepsilon_p}{K} + \rho_p\right)D_e = \frac{D_p\varepsilon_p}{K} + \rho_p D_s \tag{21}$$

To solve Eq. (20) the following initial (I.C) and boundary (B.C) conditions are stated

$$\mathrm{q} = 0, \qquad \mathrm{t} = 0 \qquad 0 < \mathrm{r} < \mathrm{r_o} \tag{22}$$

$$\mathrm{q} = \mathrm{q_{eq}}, \quad \mathrm{t} = \infty, \quad \mathrm{r} = \mathrm{r_o} \tag{23}$$

$$\frac{\partial \mathrm{q}}{\partial \mathrm{r}} = 0, \qquad \mathrm{t} > 0, \qquad \mathrm{r} = 0 \tag{24}$$

The analytical solution of Eq. (20) subject to I.C and B.C given in Eqs. (22–24), for an adsorption that follows a linear isotherm in a bath of finite volume is expressed as (30)

$$q_t = q_e\left\{1 - \sum_{n=1}^{\infty}\frac{6\alpha(\alpha+1)\exp(-\beta_n^2 D_e t/r_o^2)}{9 + 9\alpha + \beta_n^2\alpha^2}\right\} \tag{25}$$

where β_ns are the positive nonzero roots of

$$\tan \beta_n = \frac{3\beta_n}{3 + \alpha\beta_n^2} \tag{26}$$

and $\alpha = C_e/(C_o - C_e)$ represents the adsorbent load factor. The α values were 0.18, 0.29, 0.18 and 0.92 for Al-Na-HUD, Al-HUD, Al-F9, and Al-A4 zeolites, respectively. In simulating experimental data using Eq. (25), D_e is taken as a fitting parameter and its value determined by minimizing the normalized standard deviation (Δq) given by Eq. (12). And since Eq. (25) involves an infinite number of terms, trials were initially made and it was found that 50 terms (n = 50) were sufficient and used in all calculations.

Model simulations of the kinetic test results are shown in Fig. 9 by solid lines, from where the best-fit effective diffusion coefficients, D_e, were computed and are summarized in Table 4. The computed D_e values were 1.12×10^{-9}, 6.14×10^{-10}, 5.27×10^{-10}, and 6.15×10^{-10} cm^2/s for Al-Na-HUD, Al-HUD, Al-F9, and Al-A4 zeolites, respectively. Though effective diffusion coefficients of fluoride in liquid-phase adsorption are not easily available in open literature, the values found in this work are higher compared to, for example, effective diffusion coefficient of 5.5×10^{-11} cm^2/s found in a closely related study by Demarco et al. (31) using the same model Eq. (25) to simulate batch kinetic data of arsenic adsorption onto a polymeric hybrid material. For the Al-HUD, Al-F9, and Al-A4 zeolites, the fluoride diffusivities were within the same magnitude even though their uptake dependences on time were different. This is because their fractional approaches to equilibrium (q_t/q_{eq}) were nearly the same. Diffusivity of fluoride in Al-Na-HUD zeolite was higher probably as a result of a combination of larger pore and higher affinity of fluoride for Al-Na-HUD.

To explore further the relative importance of external mass transfer *vis-a-vis* internal diffusion, Biot number ($N_{Bi} = k_f\, r_o/D_e$) was considered. Table 4 summarizes the N_{Bi} values for the four zeolite adsorbents. The N_{Bi} values are significantly larger than 100 indicating that film diffusion resistance was negligible.

Desorption Studies

Adsorption is a well-established technology for water and wastewater purification. However, the success of this technology, for environmental and economic reasons, depends on the possibility of desorbing the target contaminant and reusing the adsorbent. Thus, desorption of fluoride from Al-F9 was initially carried out using acetic acid (pH 3.0), demineralized water (pH 5.7), sodium bicarbonate (pH 8.8), and sodium hydroxide (pH 12.6) desorbing agents. Acetic acid was only able to desorb 5% of the loaded fluoride and was the least effective agent for fluoride desorption, followed by demineralized water (12%) and NaOH (35.2%). The most effective solution was sodium bicarbonate (63%). From these results, it can be

deduced further that the mode of fluoride adsorption was mainly by chemisorption mechanism. For a successful operation, the desorbing agent should be effective and should not cause much damage to the adsorbent. Assuming that the mechanism of fluoride uptake was similar for all the zeolite types, sodium bicarbonate was chosen for further trials. Figure 11 shows the fluoride desorption results for Na-Al-HUD, Al-HUD, Al-F9, and Al-A4 zeolites. In the first desorption step, only 61–67 % of the bound fluoride was desorbable. Thus, several batch steps were used. It is observed that the cumulative quantity of fluoride desorbed marginally increased with each successive batch step, suggesting that application of column desorption would be more appropriate. By the 4th desorption step, the ease of fluoride desorption followed the order Al-F9 > Na-Al-HUD >Al-HUD> Al-A4.

CONCLUSIONS

Batch equilibrium and kinetic studies were undertaken to evaluate the fluoride adsorption characteristics of Al^{3+}-pretreated low-silica synthetic zeolites. The adsorbents were found to remove fluoride from water to levels below the WHO MAC value. The fluoride removal was found to be dependent on initial solution pH suggesting a chemisorption mechanism. This was further confirmed from desorption studies. In simulating equilibrium data, simple models such as F, LF, RP, and DR were used. The model parameters were obtained and discussed in relation to the adsorbents used. For kinetic studies, two modeling approaches were applied. The first approach considered chemical reaction kinetics while the second approach dealt with mass transfer processes. The chemical reaction kinetics was interpreted in terms of Elovich mechanism wherein the predicted initial fluoride uptake was found to be

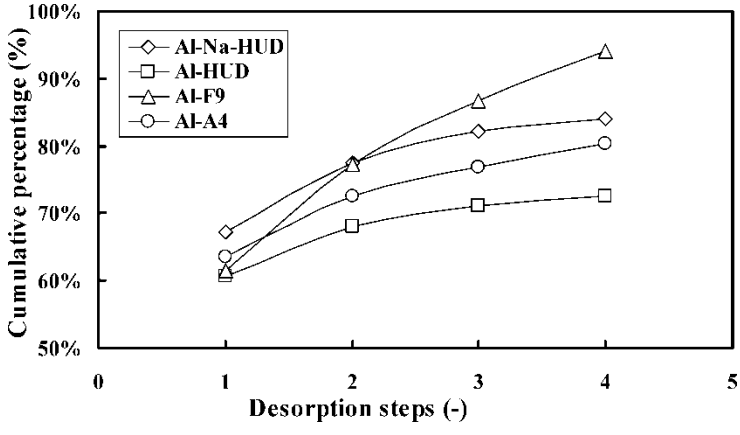

Figure 11. Desorption of fluoride from Al^{3+}-pretreated low-silica zeolites using sodium bicarbonate as a desorbing agent.

dependent on the zeolite type. Likewise, the external mass transfer process was dependent on the zeolite type and the magnitude of the external mass transfer coefficients was in the range 10^{-2}–10^{-3} cm/s. Results from intraparticle diffusion modeling demonstrated that the effective intraparticle diffusion coefficients were in the range 10^{-9}–10^{-10} cm^2/s for all the zeolites. In terms of equilibrium uptake and adsorption rates, the following performance order was observed: Al-Na-HUD > Al-F9> Al-HUD >Al-A4.

ACKNOWLEDGEMENT

The authors wish to express their sincere gratitude to Dr. Yoshitake Masuda and Prof. Kunihito Koumoto of the Department of Applied Chemistry, Nagoya University, for carrying out the zeta potential measurements. One of the authors, M.S. Onyango, thanks the Japanese Ministry of Education, Culture, Sports, Science, and Technology, for offering a scholarship for pursuing the present work.

REFERENCES

1. Majdan, M., Pikus, S., Kowalska-Ternes, M., et al (2003) Equilibrium study of selected divalent *d*-electron metals adsorption on A-type Zeolite. *J. Colloid Interface Sci.*, 262: 321.
2. García-Sánchez, A., Alastuey, A., and Querol, X. (1999) Heavy metal adsorption by different minerals: application to the remediation of polluted soils. *Sci. Total Environ.*, 242: 179.
3. Doula, M.K. and Ioannou, A. (2003) The effect of electrolyte anion on Cu adsorption–desorption by clinoptilolite. *Microporous and Mesoporous Mater.*, 58: 115.
4. Song, K.C., Lee, H.K., Moon, H., and Lee, K.J. (1997) Simultaneous removal of the radiotoxic nuclides Cs^{137} and I^{129} from aqueous solution. *Sep. Purif. Technol.*, 12: 215.
5. Dal Bosco, S.M., Jimenez, R.S., and Carvalho, W.A. (2005) Removal of toxic metals from wastewater by Brazilian natural scolecite. *J. Colloid Interface Sci.*, 281: 424.
6. Shevade, S. and Ford, R.G. (2004) Use of synthetic zeolites for arsenate removal from pollutant water. *Water Res.*, 38: 3197.
7. Elizalde-González, M.P., Mattusch, J., Einicke, W.D., and Wennrich, R. (2001) Sorption on natural solids for arsenic removal. *Chem. Eng. J.*, 81: 187.
8. Onyango, M.S., Kojima, Y., Aoyi, O., Bernardo, E.C., and Matsuda, H. (2004) Adsorption equilibrium modeling and solution chemistry dependence of fluoride removal from water by trivalent-cation-exchanged zeolite F-9. *J. Colloid Interface Sci.*, 279: 341.
9. Cortés-Martínez, R., Martínez-Miranda, V., Solache-Ríos, M., and García-Sosa, I. (2004) Evaluation of natural and surfactant-modified zeolites in the removal of cadmium from aqueous solutions. *Sep. Sci. Technol.*, 39: 2711.
10. Onyango, M.S., Matsuda, H., and Ogada, T. (2003) Sorption kinetics of arsenic onto iron-conditioned zeolite. *J. Chem. Eng. Jpn.*, 36: 477.

11. Xu, Y.H., Nakajima, T., and Ohki, A. (2002) Adsorption and removal of arsenic(V) from drinking water by aluminum-loaded Shirasu-zeolite. *J. Hazardous Mater.*, 92: 275.
12. Unesco. Trace Elements in Water and Public Health. www.iah.org/briefings/Trace/trace.htm (Accessed October, 2004).
13. Wasay, S.A., Tokunaga, S., and Park, S.W. (1996) Removal of hazardous anions from aqueous solutions by La(III)- and Y(III)-impregnated alumina. *Sep. Sci. Technol.*, 31: 1501.
14. Ho, L.N., Ishihara, T., Ueshima, S., Nishiguchi, H., and Takita, Y. (2004) Removal of fluoride from water through ion exchange by mesoporous Ti oxohydroxide J. *Colloid Interface Sci.*, 272: 399.
15. Ruixia, L., Jinlong, G., and Hongxiao, T. (2002) Adsorption of fluoride, phosphate, and arsenate ions on a new type of ion exchange fiber. *J. Colloid Interface Sci.*, 248: 268.
16. Mahramanlioglu, M., Kizilcikli, I., and Bicer, I.O. (2002) Adsorption of fluoride from aqueous solution by acid treated spent bleaching earth J. *Fluorine Chem.*, 115: 41.
17. Ramos, R.L., Ovalle-Turrubiartes, J., and Sanchez-Castillo, M. (1999) Adsorption of fluoride from aqueous solution on aluminum-impregnated carbon. *Carbon.*, 37: 609.
18. Ghorai, S. and Pant, K.K. (2004) Investigations on the column performance of fluoride adsorption by activated alumina in a fixed-bed. *Chem. Eng. J.*, 98: 165.
19. Fan, X., Parker, D.J., and Smith, M.D. (2003) Adsorption kinetics of fluoride on low cost materials. *Water Res.*, 37: 4929.
20. Ghorai, S. and Pant, K.K. (2005) Equilibrium, kinetics and breakthrough studies for adsorption of fluoride on activated alumina. *Sep. Purif. Technol.*, 42: 265.
21. Sujana, M.G., Thakur, R.S., and Rao, S.B. (1998) Removal of fluoride from aqueous solution by using alum sludge. *J. Colloid Interface Sci.*, 206: 94.
22. Wang, Y. and Reardon, E.J. (2001) Activation and regeneration of a soil sorbent for defluoridation of drinking water. *Appl. Geochem.*, 16: 531.
23. Harrington, L.F., Cooper, E.M., and Vasudevan, D. (2003) Fluoride sorption and associated aluminum release in variable charge soils. *Colloid Interface Sci.*, 267: 302.
24. Cheung, W.C., Porter, J.F., and McKay, G. (2001) Sorption kinetic analysis for the removal of cadmium ions from effluents using bone char. *Water Res.*, 35: 605.
25. House, W.A., Denison, F.H., and Armitage, P.D. (1995) Comparison of the uptake of inorganic phosphorus to a suspended and stream bed-sediment. *Water Res.*, 29: 767.
26. Lazaridis, N.K. and Asouhidou, D.D. (2003) Kinetics of sorptive removal of chromium(VI) from aqueous solutions by calcined $Mg-Al-CO_3$ hydrotalcite. *Water Res.*, 37: 2875.
27. Teng, H. and Hsieh, C. (1999) Activation energy for oxygen chemisorption on carbon at low temperatures. *Ind. Eng. Chem. Res.*, 38: 292.
28. Wang, Z., Ainsworth, C.C., Friedrich, D.M., Gassman, P.L., and Joly, A.G. (2000) Kinetics and mechanism of surface reaction of salicyclate on alumina in colloidal aqueous suspension. *Geochim. Cosmochim. Ac.*, 64: 1159.
29. McKay, G. (1983) The adsorption of dyestuffs from aqueous solutions using activated carbon. IV. External mass transfer processes. *J. Chem. Tech. Biotechnol.*, 33A: 205.
30. Crank, J. (1975) *The Mathematics of Diffusion*; 2nd Ed.; Clarenden Press: Oxford, U.K.
31. DeMarco, M.J., SenGupta, A.K., and Greenleaf, J.E. (2003) Arsenic removal using a polymeric/inorganic fhybrid sorbent. *Water Res.*, 37: 164.